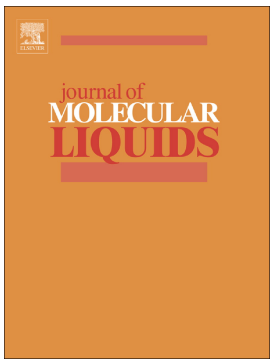

Effects of thiol functionalization of a waste-derived activated carbon on the adsorption of sulfamethoxazole from water: Kinetic, equilibrium and thermodynamic studies

Guilaine Jaria, Vânia Calisto, Maria Victoria Gil, Paula Ferreira, Sérgio M. Santos, Marta Otero, Valdemar I. Esteves

PII: S0167-7322(20)37245-7

DOI: https://doi.org/10.1016/j.molliq.2020.115003

Reference: MOLLIQ 115003

To appear in: *Journal of Molecular Liquids*

Received date: 28 July 2020

Revised date: 2 November 2020

Accepted date: 6 December 2020

Please cite this article as: G. Jaria, V. Calisto, M.V. Gil, et al., Effects of thiol functionalization of a waste-derived activated carbon on the adsorption of sulfamethoxazole from water: Kinetic, equilibrium and thermodynamic studies, *Journal of Molecular Liquids* (2020), https://doi.org/10.1016/j.molliq.2020.115003

Effects of thiol functionalization of a waste-derived activated carbon on the adsorption of sulfamethoxazole from water: kinetic, equilibrium and thermodynamic studies

Guilaine Jaria[a], Vânia Calisto[a,*] vania.calisto@ua.pt, Maria Victoria Gil[b], Paula Ferreira[c], Sérgio M. Santos[d], Marta Otero[e], Valdemar I. Esteves[a]

[a]CESAM & Department of Chemistry, University of Aveiro, Campus Universitário de Santiago, 3810-193 Aveiro, Portugal.

[b]Instituto de Ciencia y Tecnología del Carbono, INCAR-CSIC, Calle Francisco Pintado Fe 26, 33011 Oviedo, Spain

[c]CICECO, Department of Materials and Ceramic Engineering, University of Aveiro, Campus Universitário de Santiago, 3810-193 Aveiro, Portugal.

[d]CICECO, Department of Chemistry, University of Aveiro, Campus Universitário de Santiago, 3810-193 Aveiro, Portugal.

[e]CESAM, Department of Environment and Planning, Campus Universitário de Santiago, 3810-193 Aveiro, Portugal.

[*]Corresponding author.

Abstract

An activated carbon was produced from paper mill sludge (AC-P) and functionalized with thiol groups (AC-MPTMS) for the adsorptive removal of the antibiotic sulfamethoxazole (SMX) from buffered solutions prepared in ultrapure water (pH 8) and real wastewater samples. The physicochemical properties of the two materials (AC-P and AC-MPTMS) showed differences, mainly in specific surface area (S_{BET}), in the type of oxygen functional groups and in the relative percentage of sulphur groups. The adsorption results showed a decrease in the Langmuir adsorption capacity (q_m) upon an increase on temperature (15, 25 and 35 °C), varying between 113 ± 7 and

42.5 ± 0.6 mg g^{-1} for AC-P and between 140 ± 20 and 28.0 ± 1.5 mg g^{-1} for AC-MPTMS. Pseudo-second order model presented the best fit for the kinetic studies, with rate constants (k_2) increasing with temperature and varying from 0.005 ± 0.002 to 0.013 ± 0.004 g mg^{-1} min^{-1} for AC-P and from 0.006 ± 0.002 to 0.03 ± 0.01 g mg^{-1} min^{-1} for AC-MPTMS. Both adsorbents showed very similar thermodynamic parameters, with the adsorption process being spontaneous (-26 kJ mol^{-1} ≤ ΔG^o ≤ -40 kJ mol^{-1}), endothermic (69 kJ mol^{-1} ≤ ΔH^o ≤ 78 kJ mol^{-1}), and entropically favourable (356 ≤ ΔS^o ≤ 365 J mol^{-1} K^{-1}). The performance of AC-MPTMS in the removal of SMX was tested in wastewater, where the material displayed lower SMX adsorption velocity and capacity than in buffered aqueous solution (pH 8) due to competitive matrix effects.

Keywords: Organosilane grafting, Adsorptive wastewater treatment, Biowastes valorization, Emerging contaminants, Pharmaceuticals

1. Introduction

Contamination of aquatic ecosystems by pharmaceuticals raises large concern. Antibiotics, which are among the most frequently detected medicines in the environment [1], are particularly worrying due to their antimicrobial resistance effect caused by the development of antibiotic resistant bacteria and spread of antibiotic resistant genes [2]. Also, the presence of antibiotics in the aquatic environment may cause toxicity towards the living organisms in the different ecosystems [2, 3]. In the future, negative effects by antibiotics are foreseen to be enhanced since it has been reported that, from 2015 to 2020, their consumption has globally increased by 65 % [1, 4]. After consumption, antibiotics are not fully metabolized by the organism and, therefore, their unaltered form, along with active metabolites, are excreted, entering the

environment through the discharge of wastewater treatment plant (WWTP) effluents, which are amongst the main sources of antibiotic in waters bodies [2, 3, 5, 6].

Sulfamethoxazole (SMX) is an antibiotic belonging to the sulfonamides group and has been found in concentrations up to μg L^{-1} in several WWTP influents and effluents and also at ng L^{-1} levels in surface waters and even in drinking waters [1-3]. Photodegradation and biodegradation can reduce the environmental persistence of this pharmaceutical; yet the extent of these phenomena can be highly dependent of the matrix composition [7]. In fact, the "pseudo-persistent" effect caused by the continuous entrance of this, and other compounds, in the environment can pose long-term risks [7]. There are evidences that the presence of SMX in concentrations as low as μg L^{-1} may have detrimental effects to the ecosystem [8], including the microbial community [9], aquatic plants and algae [10]. This implies the necessity of implementing efficient removal technologies in WWTP treatments.

Adsorption was pointed out as a very interesting water treatment solution for both organic and inorganic contaminants [11-14]. Along with its efficacy, the advantages of adsorption also include easiness of operation, low cost, and no or lower formation of toxic by-products [4, 11, 14]. In fact, and in the particular case of organic contaminants, some studies concerning wastewater treatment at pilot-scale level, suggest adsorption as a preferable method when compared to some oxidation processes, achieving high removal efficiency [15]. Moreover, target substances, even at small concentrations and when present in complex mixtures, can be selectively adsorbed [12]. Activated carbons (AC) are generally pointed out as being very versatile materials for adsorption treatments, presenting a high surface area and being able to effectively adsorb a wide range of contaminants, including organic compounds [13, 16]. Despite the importance of high surface areas for the high adsorption capacities commonly

achieved by these materials, other properties such as pore size distribution and surface functionalities may also have a key role in the adsorptive removal of organic pollutants, since adsorption is known to be a complex process involving several phenomena [17]. Moreover, the properties of the adsorbate are also of vital importance to define adsorbent-adsorbate affinities [18]. Therefore, and considering that pharmaceuticals can present very distinct physicochemical properties, structure and molecular size, different efficiencies may be attained in the adsorptive removal of these contaminants, with adsorption capacity also depending on the applied operational conditions, such as pH, temperature, adsorbent dosage and adsorbate concentration [1, 11-13]. This is well observed in the work of Guillossou et al. [19], where an AC adsorption pilot strategy was applied as tertiary treatment. High differences were found in the removal percentages of the 25 organic micropollutants (OMP) studied, both by conventional WWTP treatments (primary and biological) and pilot advanced treatment with AC [19]. In the particular case of SMX, the removal percentage by conventional WWTP treatments was -29 (±53) % increasing only to 34 (±19) % with the pilot advanced treatment [19]. Hence, in order to improve the removal of less adsorbed OMP, the functionalization of AC may be an interesting approach [20]. A recent example of this strategy is the work of Sekulic et al. [21], where a waste lignocellulosic-based AC was functionalized aiming at the introduction of phosphorous functional groups on its surface. The functionalized AC was successfully applied in the removal of several pharmaceuticals, including SMX, in water under controlled pH 6-7 [21].

In a previous work on the effect of different surface functionalizations of a waste-derived activated carbon on the adsorption of pharmaceuticals from water [22], a thiol functionalized activated carbon (AC-MPTMS) showed potential for enhanced adsorption of SMX from wastewater relatively to other functionalized materials. In this

work, an AC (hereafter named AC-P) was produced from an industrial residue (primary paper mill sludge) [23] and then used as precursor for the synthesis of a functionalized material (AC-MPTMS), which was obtained by organosilane grafting with (3-mercaptopropyl)trimethoxysilane. Both AC-P and AC-MPTMS were characterized by nitrogen (N_2) adsorption isotherms, determination of BET surface area (S_{BET}), Fourier transform infrared with attenuated total reflectance (FTIR-ATR), X-ray photoelectron spectroscopy (XPS) and scanning electron microscopy (SEM). The adsorption of the antibiotic SMX onto AC-MPTMS was then addressed and compared to that of AC-P by analyzing the thermodynamic parameters involved in the process.

2. Experimental section

2.1. Chemicals and reagents

The production of the AC-P was achieved using potassium hydroxide (KOH, EKA PELLETS, ≥86 %) as activating agent. For the chemical functionalization, the following reagents were used: (3-mercaptopropyl)trimethoxysilane (MPTMS, Aldrich, 95 %) and toluene (Aldrich, 99.8 %). The pharmaceutical SMX (>98 %) was purchased from TCI. Di-potassium hydrogen (K_2HPO_4, PanReac AppliChem, 99.0 %), potassium dihydrogen phosphate (KH_2PO_4, MERCK, 99.5 %), and ortho-phosphoric acid (H_3PO_4, Panreac, 85.0 %) were used for pH adjustment and control.

For the analytical determination of SMX, in the aqueous phase, by Micellar Electrokinetic Chromatography (MEKC), a buffer solution of 15 mM sodium tetraborate (Riedel-de Haën) and 30 mM sodium dodecyl sulphate (SDS, Sigma-Aldrich, 99 %) was used as background electrolyte. For the capillary conditioning, 1 M sodium hydroxide (NaOH, José Manuel Gomes dos Santos, 99.3 %) and

hexadimethrine bromide (polybrene, Sigma-Aldrich) were used. Also, ethylvanillin (Aldrich, 99.0 %) was used as internal standard.

All the solutions were prepared in ultrapure water obtained from a Milli-Q Millipore system (Milli-Q plus 185).

2.2. Material synthesis and characterization

2.2.1. Production of AC-P and AC-MPTMS

Primary paper mill sludge, a waste product obtained from the primary treatment of the effluents of the pulp and paper industry, was used as raw material for the production of AC-P following the optimized procedure described in Jaria et al. [23]. Subsequently, organosilane grafting of AC-P with (3-mercaptopropyl)trimethoxysilane was performed as described in Jaria et al. [22] in order to produce AC-MPTMS. A brief description of the experimental procedures for the production of AC-P and AC-MPTMS is presented in Supplementary Material (SM).

2.2.2. Physicochemical characterization of the carbon materials

The physicochemical characterization of AC-P and AC-MPTMS was performed by the determination of S_{BET} and microporous volume (W_0), Fourier transform infrared spectroscopy with attenuated total reflectance (FTIR-ATR), X-ray photoelectron spectroscopy (XPS), and scanning electron microscopy (SEM).

The S_{BET} and W_0 of AC-P and AC-MPTMS were determined by the nitrogen (N_2) adsorption isotherms that were acquired at 77 K using an ASAP 2420 from Micromeritics Instrument Corporation. The S_{BET} values of both materials were calculated using the Brunauer–Emmett–Teller equation [24] in the relative pressure range 0.01–0.1 and the respective total pore volumes (V_p) were assessed from the

amount of nitrogen adsorbed at a relative pressure of 0.99. W_0 was determined by the application of the Dubinin–Radushkevich equation [25] or the Dubinin-Astakhov (DA) equation to the lower relative pressure zone of the nitrogen adsorption isotherm.

The FTIR-ATR spectra were obtained in a IRaffinity-1 equipment (Shimadzu), using an ATR module, under a nitrogen purge, by film deposition of the AC materials. The film deposition consisted of placing a drop of an AC suspension (in water) on the ATR crystal followed by drying with N_2 until a film is formed over the crystal. The measurements were performed in the wavenumber range of 700–4000 cm^{-1}, with 128 scans, 4 cm^{-1} of resolution and with atmosphere correction.

The XPS analysis was performed in an ultra-high vacuum (UHV) system with a base pressure of 2×10^{-10} mbar equipped with a hemispherical electron energy analyzer (Phoibos 150, SPECS), a delay-line detector and a monochromatic Al Kα (1486.74 eV) X-ray source. High resolution spectra were recorded at normal emission take-off angle and with a pass-energy of 20 eV, providing an overall instrumental peak broadening of 0.5 eV.

The SEM images were obtained in a SU-70 equipment (Hitachi) at magnifications of 3 000, 10 000, 30 000 and 50 000 x.

2.3. Adsorption studies

Using AC-P and AC-MPTMS as adsorbents, kinetic and equilibrium studies on the adsorption of SMX were performed in batch mode and under stirring at 80 rpm in an overhead shaker (Reax 2, Heidolph Instruments). Experiments with ultrapure water were carried out at three different temperatures (15, 25 and 35 ºC) and at buffered pH 8, which was chosen to be close to the pH of wastewater. For the pH adjustment, SMX solutions were prepared in phosphate buffer 0.01 M using 94 mL of 0.1 M K_2HPO_4 and

6 mL of 0.1 M KH_2PO_4 for 1 L of solution. When necessary, H_3PO_4 1M or KOH 1M were used to tune the final pH.

The adsorptive performance of AC-MPTMS was also assessed in an effluent from a local WWTP that treats domestic sewage. For that purpose, batch adsorption experiments under constant stirring (80 rpm) were carried out at 25 °C using SMX solutions prepared in wastewater collected in May 2019 at the outlet of the WWTP after secondary decanting, which corresponds to the effluent that is discharged into the aquatic environment. After collection, wastewater was filtered through 0.45 µm, 293 mm membrane filters (Gelman Sciences) and stored at 4 °C if not immediately used after filtration. Wastewater was characterized for conductivity (HI763100, Hanna Instruments), pH (HI11310, Hanna Instruments) and TOC (TOC-V_{CPH}, SSM-5000A (Shimadzu)).

2.3.1. Kinetic studies

Kinetic studies were performed to determine the time needed to reach the equilibrium (t_e) for the adsorption of SMX onto AC-P and AC-MPTMS. For experiments in buffered solutions prepared in ultrapure water (pH 8), solutions of SMX with an initial concentration, C_0 (mg L^{-1}), of 5 mg L^{-1} were placed in polypropylene tubes in presence of the adsorbent at a concentration of 0.040 g L^{-1}. The C_0 (mg L^{-1}) used in this work, which is higher than SMX concentrations typically found in wastewater, was selected for practical reasons, namely for being possible to weigh with accuracy a mass of adsorbent that allows for a significant SMX adsorption but also a measurable residual concentration of the antibiotic after adsorption. Also, and considering the real application of the adsorbent for water treatment, the determination of the isotherms parameters, even at relatively high concentrations of adsorbate, allows

to predict or estimate the probable amount of adsorbent required to achieve a determined percentage of removal of a contaminant [26].

The polypropylene tubes were stirred under controlled temperature, for different time intervals ranging from 5 min to 480 min. Regarding the study on the SMX adsorption onto AC-MPTMS from wastewater, kinetic experiments were performed as previously described but with an adsorbent concentration of 0.060 g L^{-1} and stirring times ranging between 15 and 1440 min. At the end of each time interval, stirring was stopped and the solutions were filtered through 0.22 µm PVDF filters (Whatman) and analyzed for the residual concentration of SMX at the corresponding time, C_t (mg L^{-1}), by MEKC, as described in SM. The adsorbed concentration of SMX onto AC-P or AC-MPTMS at a time t, q_t (mg g^{-1}), was calculated by a mass balance. All the adsorption kinetic experiments were performed in triplicate and in parallel with controls (tubes without adsorbent). Fittings of experimental results to the kinetic pseudo-first order model (PFO) [27] and pseudo-second order model (PSO) [28] equations, which are presented in Table S1 in SM, were determined using GraphPad Prism, version 5.

2.3.2. Equilibrium studies

Equilibrium studies were carried out to determine the adsorbents behavior and capacities at the equilibrium and the corresponding equilibrium constant. Hence, for experiments from buffered solutions prepared in ultrapure water (pH 8), predefined volumes of SMX solution with a C_0 (mg L^{-1}) of 5 mg L^{-1} were placed in polypropylene tubes together with different concentrations of AC-P or AC-MPTMS, ranging from 0.020 g L^{-1} to 0.300 g L^{-1}. The polypropylene tubes were stirred under controlled temperature during the equilibrium time, t_e (min), determined in the previous kinetic studies. Regarding the SMX adsorption onto AC-MPTMS from wastewater, the

equilibrium study was performed as described above but with adsorbent concentrations ranging from 0.040 to 0.400 g L^{-1}. After the corresponding equilibrium time, stirring was stopped and solutions were filtered through 0.22 µm PVDF filters (Whatman) and analyzed for the equilibrium concentration of SMX, C_e (mg L^{-1}), by MEKC, as described in SM. The adsorbed concentration of SMX onto AC-P or AC-MPTMS at the equilibrium, q_e (mg g^{-1}), was calculated by a mass balance. All the adsorption equilibrium experiments were performed in triplicate, together with control tubes without adsorbent. Fittings of equilibrium experimental results to the isotherm models of Langmuir and Freundlich, which are depicted in Table S1 in SM, were determined using GraphPad Prism, version 5.

2.5. Adsorption activation energy and thermodynamic parameters

Activation energy (E_a) is an important thermodynamic parameter representing the minimum energy necessary for a specific interaction between the adsorbate and the adsorbent to occur [29]. The calculation of E_a allows one to determine the dependence of the adsorption reaction rate on temperature [30]; E_a can be determined by applying Arrhenius equation (equation 1) [30]:

$$\ln k = -\frac{E_a}{R}\frac{1}{T} + \ln A \qquad (1)$$

where k is the adsorption rate constant, T (K) is the temperature and A is the frequency factor or collision probability factor [29, 31]. By plotting ln k *vs* 1/T, E_a was determined from the slope and A from the intercept.

Thermodynamic parameters, namely the standard Gibbs energy ($\Delta G°$, J mol^{-1}), standard enthalpy ($\Delta H°$, J mol^{-1}) and standard entropy ($\Delta S°$, J mol^{-1} K^{-1}), associated to the adsorption of SMX onto AC-P and AC-MTPS was calculated on the basis of the

third principle of thermodynamics (equation 2) and the Van't Hoff equation (equation 3) [32, 33]:

$$\Delta G° = \Delta H° - T\Delta S° \qquad (2)$$

$$\Delta G° = -RT \ln (K_e°) \qquad (3)$$

where R is the perfect gas constant (8.314 J K^{-1} mol^{-1}) and K_e is the thermodynamic equilibrium constant (dimensionless) [32, 33]. The combination of the equations above (2 and 3) results in equation 4, which allows for the determination of the thermodynamic parameters $\Delta H°$ and $\Delta S°$ [32, 34].

$$\ln K_e^\circ = -\frac{\Delta H^\circ}{R}\frac{1}{T} + \frac{\Delta S^\circ}{R} \qquad (4)$$

By plotting ln ($K_e°$) *versus* 1/T, ΔH^o was determined from the slope and $\Delta S°$ from the intercept. The adsorption equilibrium constant derived from the fittings of experimental results to isotherm models must be a dimensionless variable, so to be possible its utilization in the Van't Hoff equation. Thus, $K_e°$ (dimensionless) was calculated using equation 5, as proposed by Lima et al. [33]

$$K_e^\circ = 1000\, K_g.MW.[Adsorbate]^\circ \frac{}{\gamma} \qquad (5)$$

where K_g (L mg^{-1}) is the Langmuir equilibrium constant for the best equilibrium fitting; MW (g mol^{-1}) is the molecular weight of the adsorbate; [*Adsorbate*]° is the standard concentration of the adsorbate (1 mol L^{-1}); and γ is the coefficient of activity of the adsorbate (dimensionless) [33]. In general, the standard concentration of a solute in a solution is considered 1 mol L^{-1}, and the activity coefficient is considered unitary for diluted solutions [33, 35]. Taking into account that the initial concentration of SMX is 5 mg L^{-1}, which is equivalent to ~2 x 10^{-5} mol L^{-1}, and that a solution is considered diluted when its molar concentration is not higher than 0.01 M [32], the SMX solution used can be seen as a very diluted solution and, therefore, the activity coefficient was considered unitary.

3. Results and Discussion

3.1. Physicochemical characterization of AC-P and AC-MTPMS

3.1.1. Specific Surface Area

The S_{BET} values obtained for AC-P and AC-MPTMS were 1433 and 1164 $m^2 g^{-1}$, respectively (Table S2). These results evidenced a reduction of 19% in the S_{BET} of the parent material after functionalization. Both AC-P and AC-MTPMS showed a high degree of microporosity (Table S2), with AC-MPTMS presenting a decrease in the micropore volume (W_o) and a slight increase in the average pore diameter, as compared to AC-P (Table S2). The pore size distribution (PSD) of the materials, represented in Figure 1, showed very similar patterns, with most of the pore volumes in the range of 2 to 4 nm. Still, AC-MPTMS displayed a slight decrease in this range as compared with AC-P, which was also observed in Jaria et al. [22], and should be related with the introduction of functional groups into the pore channels of AC-P.

3.1.2. Scanning electronic microscopy (SEM)

The SEM images for AC-P and AC-MPTMS are depicted in Figure S1. Both materials present a high degree of porosity, which is in accordance with the S_{BET} results, with AC-P presenting a rougher and more porous surface than AC-MPTMS. This last observation may be related to the surface modification with the organosilane precursor, which smoothed the AC surface.

3.1.3. Fourier Transform Infrared with Attenuated Total Reflectance (FTIR-ATR)

The FTIR-ATR spectra obtained for AC-P and AC-MPTMS are presented in Figure S2 in SM. The FTIR-ATR spectra of both materials are very similar presenting a

main peak of absorbance around 1510 cm^{-1}, which can be assigned to aromatic ring stretch (C=C–C) [36]; a small signal at 1645 cm^{-1}, which can be associated to carbon double bond stretch (C=C); and three small peaks between 3500 and 3900 cm^{-1}, which may be mostly assigned to hydroxyl groups (OH stretch) [36]. AC-MPTMS spectrum shows a slight band around 1112 cm^{-1}, which may correspond to sulphur in the form of sulfonates or due to the presence of organic siloxane (Si–O–C) [36], possibly from unreacted MPTMS during the synthesis of AC-MPTMS. Yet, FTIR analysis did not evidenced the presence of a band around 2560 cm^{-1}, typical of thiol groups [37-39]. However, FTIR spectra obtained for AC are commonly characterized by wide absorbance bands with low resolution, which can make difficult the identification of specific and low intensity peaks. The levels of condensation of aromatic rings may influence this trend due to the absorption of infrared radiation [40]. In order to get a more detailed characterization on the surface chemistry of the produced materials, XPS analysis was also carried out, results being next displayed.

3.1.4. X-Ray photoelectron spectroscopy (XPS)

XPS high-resolution spectra are presented in Figure 2, while the overview spectra and the results from the XPS analysis of AC-P and AC-MPTMS can be seen in Figure S3 and Table S3 (in SM), respectively.

Inspection of the XPS overview spectra and the high resolution spectra for C1s, N1s and Si2s+S2p, allows to observe that AC-P and AC-MPTMS present similar profiles, just with the Si2s+S2p spectra revealing differences on the intensities of the peaks associated to sulphur bonds (around 163 and 164 eV) (Figure 2 and Figure S3 in SM). In what concerns the high-resolution spectra, and for C1s, both materials present a main peak at 284.5 eV assigned to the graphitic carbon (sp^2) [41], followed by a peak

around 285.3-285.5 eV attributed to C–C on the edge of graphene sheets (sp^3), C–H bonds [41], and/or to C–OH groups [42]. The other peaks may be associated to other functionalities such as carbon-oxygen single bond in ether and alcohol groups (~286 eV) [41, 43]; double bond carbon-oxygen groups (–C=O) [41, 44] or –C=N– species [45] around 287 eV; carbon in carboxyl, lactone or ester groups (~ 288 eV) [43]; and carbon in carbonate groups [43] (Figure 2 and Table S3 in SM). In the case of nitrogen, it is possible to observe in the overview spectra (Figure 2), that the peak associated to the nitrogen core-level is very small, nearly imperceptible (Figure S3 in SM). Nevertheless, the high-resolution N1s spectra show the same pattern for both AC-P and AC-MPTMS, presenting three peaks that can be assigned to pyridinic nitrogen (~397-398 eV); pyrrolic or pyridonic nitrogen (~400 eV); and quaternary nitrogen (~401-402 eV) [45, 46]. The main differences are in the relative percentage of each group, with AC-P presenting a higher percentage for pyridinic and pyrrolic nitrogen than AC-MPTMS, while AC-MPTMS has a greater percentage of quaternary nitrogen than AC-P (Figure 2 and Table S3 in SM). For the Si2s+S2p high-resolution spectra, it is evident the relatively large peak associated to the sulphur binding energies for AC-MPTMS (Figure 2 and Table S3 in SM). Furthermore, both AC-P and AC-MPTMS present a high peak corresponding to silanes around 154 eV [47]; two peaks around 163 and 164 eV, which have a higher relative percentage for AC-MPTMS (Table S3 in SM), and may be respectively attributed to S–H, S–C bonds and thiol moieties [48], and to S–S bonds [47], elemental S and thiol groups [48]; and a fourth peak at 168-169 eV, which may be assigned to sulfoxide groups [48]. In what concerns the high resolution O1s spectra, large differences may be observed between the materials, with AC-MPTMS presenting only one peak at 532.3 eV, which is mostly associated to single bonded carbon-oxygen groups (C–O–C and C–OH) [45, 46]. In the case of AC-P, the O1s

spectrum shows a peak at 532.8 eV, with the highest relative percentage (71.6%); another at 531.0 eV, which is possibly due to the presence of double bond oxygen groups (C=O) [46] in quinones [41] or in carbonyl and carboxylic groups [41, 42]; and a third one at 534.0 eV, which can be assigned to oxygen in carboxyl groups (–COOH or COOR) [41] or to ether and hydroxyls bonded to aromatics [42] (Figure 2 and Table S3 in SM).

As for results shown in this section, the chemical characterization of the adsorbent, performed by XPS and FTIR-ATR analyses, showed differences between the parent and the functionalized materials. In particular, it is to highlight that XPS analysis evidenced intensity differences in the peaks of S2p+S2s, which are related to the sulphur binding energies, and were larger for AC-MPTMS than for AC-P. Also, textural changes due to thiol functionalization were clearly observed in N_2 adsorption isotherms (for S_{BET} determination) and SEM images of AC-MPTMS as compared with AC-P.

3.2. Kinetic and equilibrium studies for the adsorption of SMX onto the AC-P and AC-MPTMS

The results of the kinetic studies on the adsorption of SMX onto AC-P and AC-MPTMS from buffered solution prepared in ultrapure water (pH 8) are presented in Figure 3 a-1 and b-1, respectively, and Table 1. Also, the fittings for the two models used (PFO and PSO) are depicted together with experimental results in Figure S4 in SM.

As it may be seen in Figure 3, kinetic curves showed a quite fast adsorption of SMX onto AC-P and AC-MPTMS, with a steep initial slope and q_t values rapidly reaching stabilization at the corresponding q_e. As for the effect of temperature, slightly steeper slopes but lower q_e may be observed for increasing temperature. For all the

studied systems, equilibrium was attained within 120 min, which was considered as the minimum t_e for the subsequent equilibrium studies.

According to results in Table 1, the PSO model presents the best correlation coefficients (R^2) for the fittings to the kinetic results. This model points to a strong interaction between adsorbate and adsorbent, not only due to the microporosity, but also due to the complementary interaction present in both entities [49]. Parameters in Table 1 evidence that, under the experimental conditions used, the fitted values of q_e decrease with temperature for both adsorbents, with those of AC-P being larger than those of AC-MPTMS. Meanwhile, the kinetic constant rates (k_2) increase with temperature, indicating a decrease in the time required to reach equilibrium [21]. Also, the obtained k_2 are very similar for both adsorbents, being only slightly higher for AC-MPTMS than for AC-P. In any case, the determined values of k_2 are similar to values recently obtained by other authors for the adsorption of SMX onto AC. For example, the adsorption of SMX at 25 °C occurred with a k_2 of 0.008 g mg^{-1} min^{-1} onto a core-shell AC [50] and of 0.0039 g mg^{-1} min^{-1} onto a cetyltrimethylammonium bromide (CTAB) modified AC [51]. On the other hand, Tonucci et al. [52] determined k_2 values for the adsorption of SMX onto an AC produced from pine tree that, as in this work, increased with increasing temperature, with values $0.001 < k_2 < 0.01$ g mg^{-1} min^{-1} in the range of 15 to 45 °C. Such an increase is in agreement with Arrhenius equation (1) and must be related to the increased mobility of SMX molecules and the increasing number of molecules with sufficient energy to undergo interaction with active sites on the adsorbents' surface.

The results from the equilibrium studies on the adsorption of SMX onto AC-P and AC-MPTMS from buffered solutions (pH 8), at different temperatures, are presented in Figure 3 a-2 and b-2, respectively, and Table 1. Also, the isotherm fittings

for the two models used (Langmuir and Freundlich) are depicted together with experimental results in Figure S5 in SM. Observing Figure 3 a-2 and b-2, and Figure S5 (in SM), AC-P and AC-MPTMS show distinct patterns, with AC-P isotherms achieving a clear *plateau*, which is not so well defined for AC-MPTMS, especially at 15 °C. This is reflected in the fitting parameters (Table 1), since AC-MPTMS at 15 °C is the only system for which the Freundlich isotherm model presents a slightly better correlation coefficient (R^2) than the Langmuir model. Also, it can be seen in Figure 3b-2 that in the low range of C_e (< 1 mg L^{-1}), AC-MPTMS displayed closer q_e at the different temperatures than AC-P (Figure 3a-2).

Considering the fitting results depicted in Table 1, the Langmuir model was selected as the most adequate for subsequent considerations on the equilibrium of the studied systems. For both AC-P and AC-MPTMS, the Langmuir constant (K_L) increases with temperature while the maximum adsorption capacity decreases. Therefore, although the affinity between SMX molecules and these adsorbents increases with temperature, the contrary occurs for the monolayer capacity. Comparing the adsorbents produced in this work, the K_L values determined for AC-P are higher than those of AC-MPTMS (Table 1), and steeper isotherms were observed for AC-P (Figure 3a-2) comparatively to AC-MPTMS (Figure 3b-2). With respect to the q_m values determined for AC-P at 25 and 35 °C, these are higher than those determined for AC-MPTMS. Meanwhile, at 15 °C, and due to the high standard deviation of the q_m values determined for AC-MPTMS, there are not significant differences between the monolayer capacity of both materials.

Differences in the obtained results on the adsorption of SMX onto AC-P and AC-MPTMS may be, in part, related with the larger S_{BET} of the former. The larger K_L and q_m determined for AC-P may be associated to the larger number of available

oxygen functional groups, like carbonyl and carboxyl groups, in comparison to AC-MPTMS. These additional groups will likely stabilize the interaction of AC with SMX through n-π electron donor-acceptor interactions and dipole-dipole H-bond [21]. As for the sulphur functional groups in AC-MPTMS, they do not seem to have significantly influenced the adsorption of SMX.

For comparison purposes, published results on the adsorption of SMX by different AC in the literature are depicted in Table S5 (within SM). Among the referred works, Sekulic et al. [21] used a lignocellulosic waste-based functionalized AC and determined a q_m of 17 mg L^{-1} (at pH 6-7 and 22 °C), which is lower than that attained by AC-MPTMS under similar conditions (at pH 8 and 25 °C). However, the commercial GAC used in the work of Moral-Rodríguez et al. [53] provided a q_m of 213, 269 and 317 mg L^{-1} at pH 7, 9 and 11, respectively (at 25 °C), which are significantly higher than those obtained in this work for both AC-P and AC-MPTMS (Table S5 in SM).

3.3. Activation energy and thermodynamic parameters for adsorption studies in buffered solutions (pH 8) prepared in ultrapure water

The E_a values associated to the adsorption of SMX onto AC-P and AC-MPTMS, which were calculated by plotting ln k_2 *vs.* 1/T (according to equation 1; Figure S6 in SM) and are depicted in Table 2, were 36 ± 13 and 61 ± 17 kJ mol^{-1}, respectively. However, according to the *t*-Student test (*t*-test) for comparing the slope of the obtained regressions presented in Figure S6 (in SM), these are not significantly different at a 5% level, with the *t* experimental value (t_{exp}) being lower than the theoretical (or critical) *t* value (t_{crit}) [54] (Table S4, in SM). In any case, as for the E_a standing between 8.4 and 83.7 kJ mol^{-1}, activated chemisorption, which involves stronger adsorption forces than physisorption, may be inferred [30, 55]. With respect to the pre-exponential factor *A*,

which can be regarded as a collision probability factor [29], it has a very high value for AC-MPTMS ($5.6 \times 10^8 \pm 6.3 \times 10^4$) comparing to that of AC-P ($1.6 \times 10^4 \pm 2.9 \times 10^2$) (Table 2).

For the determination of thermodynamic parameters, the calculation of $K_e°$ was performed according to equation (5), where, considering the selection of Langmuir fittings to describe the experimental data (see section 3.2), K_g was equaled to K_L. Then, ln $K_e°$ was plotted vs. 1/T (according to equation 4; Figure S7 in SM). These plots allowed for the determination of $\Delta H°$, $\Delta S°$ and $\Delta G°$, which are depicted in Table 2. As it may be observed, for both AC-P and AC-MPTMS, the adsorption of SMX is a spontaneous process at the temperatures considered, since $\Delta G°$ presented negative values [56, 57]. Furthermore, for both materials, a slight decrease of the $\Delta G°$ values with the temperature was observed, indicating that the increase of the temperature is favorable for the spontaneity of SMX adsorption. As for the increasing K_L with temperature (Table 1), $\Delta H°$ inferred from equation (4), presented positive values, viz. 68.9 and 78.2 kJ mol^{-1}, respectively for AC-P and AC-MPTMS, indicating the endothermic nature of the adsorption of SMX onto these materials. Endothermic adsorption ($\Delta H° > 0$), which absorbs energy in the form of heat from its surroundings, is unequivocally attributable to chemisorption (although chemisorption is frequently exothermic, physisorption is always an exothermic process) [58, 59]; this is in accordance with what was inferred from the values determined for E_a. Endothermicity may be related with the dissociation of SMX molecules on chemisorption, with the dissociation energy being greater than the energy of bond formation with the surface. Consequently, since $\Delta G°$ accompanying any spontaneous process, as it is this case, is negative, endothermic adsorption always implies a positive entropy change. Indeed, $\Delta S°$ presented positive values for both systems, 356 ± 88 J mol^{-1} K^{-1} and 365 ± 96 J mol^{-1} K^{-}

[1], AC-P and AC-MPTMS, respectively, which is in agreement with a dissociative mechanism [58].

$\Delta G°$ values similar to those obtained in this work, namely around -38 kJ mol^{-1} [52] and -24 kJ mol^{-1} [51], have been respectively published for the adsorption of SMX onto pine tree AC and CTAB modified AC at temperatures within 288 and 318 K (Table S5 in SM). These authors [51, 52] also found that SMX adsorption onto the produced adsorbents implied an increase of entropy, but, contrarily to this work, the process was exothermic.

3.4. Evaluation of AC-MPTMS in the adsorption of SMX from wastewater

The thiol functionalized material AC-MPTMS was tested for the adsorption of SMX from an effluent of a local WWTP. The characterization of the used wastewater was as follows: pH of 7.99, conductivity of 3.03 mS cm^{-1}, and a total organic content of 21.5 mg L^{-1}.

Kinetic and equilibrium results on the adsorption of SMX from the real matrix onto AC-MPTMS are presented in Figure 4a and b, respectively, together with fittings to the considered models, while the fitted parameters are depicted in Table 3. By the kinetic fitting in Figure 4a, it may be observed that q_t rapidly increases at the initial part of the curve and that the adsorption equilibrium is attained around 240 min. Comparing with the results obtained in ultrapure water buffered solutions (Figure 3b-1), the increase in the time necessary for reaching the equilibrium in the effluent is clear. This is also seen by the value estimated for the rate constant, k_2, of PSO model (presenting the best fit correlation, Table 3), which is around half of the value obtained in buffered ultrapure water (pH 8) at 25 °C (Table 2).The values obtained for q_e by the PSO model in wastewater were also smaller than the ones obtained in buffered solutions (pH 8).

Such a decrease in both q_e and k_2 may be related with the matrix effects in wastewater, namely, due to the presence of dissolved organic matter (DOM) [4]. A decrease of the fitted q_e accompanied by an increase of k_2 has been observed in some studies for the adsorption of other pharmaceuticals [60] and specifically for SMX [61] from wastewater, as compared with ultrapure water and for waste-based adsorbents. In any case, the k_2 and fitted q_e in Table 3 show that adsorption of SMX onto AC-MPTMS from wastewater was faster than SMX adsorption onto the functionalized biochar produced by Ahmed et al. [62] when used in synthetic wastewater at pH 4-4.25 (k_2 = 0.0002 g mg^{-1} min^{-1}, q_e = 12.15 mg g^{-1}).

Relatively to the equilibrium study, the best isotherm model that fit the experimental data is the Langmuir model, predicting a maximum adsorption capacity of (16.1 ± 0.3) mg g^{-1} and a K_L of (3.8 ± 0.4) L mg^{-1} (Table 3 and Figure 4b). In Figure 4b, the tendency for the formation of a *plateau* can be observed, corresponding to the monolayer adsorption. It is observed a great reduction in the Langmuir adsorption capacity in wastewater as compared with buffered solutions at pH 8 prepared in ultrapure water, namely from 48.9 ± 1.4 (Table 1) to 16.1 ± 0.3 mg g^{-1} (Table 3). Therefore, it may be concluded that the sulphur functionalization of AC-P did not result in a material with increased performance in wastewater. In any case, despite the lower value obtained in the wastewater matrix, the here obtained q_m is in the same range as the determined for the functionalized AC produced by Sekulic et al. [21], which was applied in ultrapure water at pH 6-7 (Table S5 in SM). Moreover, the decrease of the adsorption capacity of AC towards micropollutants (including SMX) in wastewater as compared with ultrapure water has already been verified by other authors [60, 61, 63] and associated to adverse effects of competing wastewater matrix components on the adsorption of target micropollutants. Using ultrapure buffered water (pH 8.1) as

reference, Bonvin et al. [63] verified two to three-fold lower adsorption capacities for the adsorption of pharmaceuticals onto powder AC from wastewater effluent (pH 7.8 ± 0.2). This reduction was especially evident in the case of pharmaceuticals showing a low carbon affinity, such as SMX [63]. Even at acidic pH, which favors SMX adsorption, Akpotu, Moodley [64] observed a decrease in the percentage of adsorption of this antibiotic by silica nanotubes graphene oxide (SNTGO) from real matrices, namely lake water and WWTP effluent. As already pointed out, background organic matter in wastewater reduces the number of adsorption sites available for micropollutants, either through direct competition for adsorption sites and/or pore blocking, and consequently decreases the adsorption efficiency of AC [4, 63].

4. Conclusions

In this work, a functionalization of a waste-based activated carbon (AC-P) was performed in order to introduce thiol groups onto its surface, to obtain AC-MPTMS, and to study the effect of such functionalization on the adsorption of SMX. The physicochemical characterization of the AC-P and AC-MPTMS showed that these materials were quite similar except for differences concerning S_{BET}, types of oxygen functional groups and the relative percentage of sulphur groups. The kinetic adsorption results in buffered solutions prepared in ultrapure water (pH 8) were described by the PSO model, with k_2 values varying between 0.005 and 0.013 g mg^{-1} min^{-1} for the adsorption of SMX onto AC-P and between 0.006 and 0.03 g mg^{-1} min^{-1} for the adsorption of SMX onto AC-MPTMS. These values allowed for the estimation of the SMX adsorption activation energy as 36 and 61 kJ mol^{-1} for AC-P and AC-MPTMS, respectively. The equilibrium results were described by the Langmuir model, with AC-P presenting maximum adsorption capacities at 15, 25 and 35 °C , of 113, 62, and 42.5

mg g^{-1}, respectively; and for AC-MPTMS of 140, 48.9, and 28.0 mg g^{-1}, respectively. The thermodynamic parameters $\Delta G°$, $\Delta H°$, and $\Delta S°$, estimated from the equilibrium constants, pointed to chemisorption as the mechanism for SMX removal by AC-P and AC-MPTMS, with both materials presenting a spontaneous, endothermic, and entropically favorable adsorption of this antibiotic. The application of AC-MPTMS to real wastewater matrix showed a decrease of the performance of this material in the adsorption of SMX as compared to solutions prepared in ultrapure water. Hence, this study revealed that the specific surface area was determinant in the performance of the produced materials regarding the adsorption of SMX, playing a more decisive role than the proposed functionalization route. Indeed, the applied functionalization did not allow for overcoming the competitive effects of background organic matter in the adsorption of SMX from wastewater, with AC-P being the most interesting material for further applications as it combines slightly higher performance with simpler production procedures.

Acknowledgements

Thanks are due to FCT/MCTES for the financial support to CESAM (UIDP/50017/2020+UIDB/50017/2020) and CICECO-Aveiro Institute of Materials, (UIDB/50011/2020 & UIDP/50011/2020), through national funds. Guilaine Jaria thanks for her PhD grant (SFRH/BD/138388/2018) supported by national funds and FSE through Fundação para a Ciência e a Tecnologia (FCT), POCH (Programa Operacional Capital Humano) and European Union. Marta Otero, Paula Ferreira and Sérgio Santos thank FCT for the Investigator Program (IF/00314/2015, IF/00300/2015 and IF/00973/2014, respectively). Vânia Calisto is thankful to FCT for Scientific Employment Stimulus (CEECIND/00007/2017). María V. Gil acknowledges support

from a Ramón y Cajal grant (RYC-2017-21937) by the Spanish Government, co-financed by the European Social Fund (ESF). The authors thank to the project RemPharm (PTDC/AAG-TEC/1762/2014) funded by FCT, I.P., through national funds, and the co-funding by the FEDER, within the PT2020 Partnership Agreement and Compete 2020. Milton Fontes and workers of Aveiro's WWTP (Águas do Centro Litoral) are gratefully acknowledged for assistance on the effluent sampling campaigns.

Credit Author Statement

Guilaine Jaria: Investigation; Conceptualization; Formal analysis; Writing - Original Draft. **Vânia Calisto**: Conceptualization; Supervision; Writing - Review & Editing; Funding acquisition. **Maria V. Gil:** Investigation; Writing - Review & Editing. **Paula Ferreira:** Resources; Writing - Review & Editing. **Sérgio M. Santos:** Resources; Writing - Review & Editing. **Marta Otero:** Conceptualization; Supervision; Writing - Review & Editing; **Valdemar Esteves:** Conceptualization; Supervision; Writing - Review & Editing;

Declaration of interests

☒ The authors declare that they have no known competing financial interests or personal relationships that could have appeared to influence the work reported in this paper.

Supplementary data

Supplementary material

References

1. Patel M, Kumar R, Kishor K, Mlsna T, Jr. CUP, Mohan D. Pharmaceuticals of Emerging Concern in Aquatic Systems: Chemistry, Occurrence, Effects, and Removal Methods. Chem Rev. 2019;119:3510−673.

2. Felis E, Kalka J, Sochacki A, Kowalska K, Bajkacz S, Harnisz M, Korzeniewska E. Antimicrobial pharmaceuticals in the aquatic environment - occurrence and environmental implications. European Journal of Pharmacology. 2020;866:172813. doi:doi:10.1016/j.ejphar.2019.172813.

3. Carvalho IT, Santos L. Antibiotics in the aquatic environments: A review of the European scenario. Environ Int. 2016;94:736-57. doi:10.1016/j.envint.2016.06.025.

4. Prasannamedha G, Kumar PS. A review on contamination and removal of sulfamethoxazole from aqueous solution using cleaner techniques: Present and future perspective. Journal of Cleaner Production. 2020;250:119553. doi:doi.org/10.1016/j.jclepro.2019.119553.

5. Grenni P, Ancona V, Barra Caracciolo A. Ecological effects of antibiotics on natural ecosystems: A review. Microchemical Journal. 2018;136:25-39. doi:10.1016/j.microc.2017.02.006.

6. Heo J, Yoon Y, Lee G, Kim Y, Han J, Park CM. Enhanced adsorption of bisphenol A and sulfamethoxazole by a novel magnetic CuZnFe2O4–biochar composite. Bioresource Technology. 2019;281:179-87.

7. Patrolecco L, Rauseo J, Ademollo N, Grenni P, Cardoni M, Levantesi C, Luprano ML, Caracciolo AB. Persistence of the antibiotic sulfamethoxazole in river water alone or in the co-presence of ciprofloxacin. Science of The Total Environment. 2018;640-641:1438-46. doi:doi:10.1016/j.scitotenv.2018.06.025.

8. Grenni P, Patrolecco L, Rauseo J, Spataro F, Lenola MD, Aimola G, Zacchini M, Pietrini F, Baccio DD, Stanton IC, Gaze WH, Caracciolo AB. Sulfamethoxazole

persistence in a river water ecosystem and its effects on the natural microbial community and Lemna minor plant. Microchemical Journal. 2019;149:103999.

9. Danner M-C, Robertson A, Behrends V, Reiss J. Antibiotic pollution in surface fresh waters: Occurrence and effects. Science of The Total Environment. 2019;664:793-804. doi:doi.org/10.1016/j.scitotenv.2019.01.406.

10. Kovalakova P, Cizmas L, McDonald TJ, Marsalek B, Feng M, Sharma VK. Occurrence and toxicity of antibiotics in the aquatic environment: A review. Chemosphere. 2020;251:126351. doi:doi.org/10.1016/j.chemosphere.2020.126351.

11. Kumar V, Saharan P, Sharma AK, Umar A, Kaushal I, Mittal A, Al-Hadeethi Y, Rashad B. Silver doped manganese oxide-carbon nanotube nanocomposite for enhanced dye-sequestration: Isotherm studies and RSM modeling approach. Ceramics International. 2020;46(8, Part A):10309-19. doi:doi.org/10.1016/j.ceramint.2020.01.025.

12. Anastopoulos I, Pashalidis I, Orfanos AG, Manariotis ID, Tatarchuk T, Sellaoui L, Bonilla-Petriciolet A, Mittal A, Núñez-Delgado A. Removal of caffeine, nicotine and amoxicillin from (waste)waters by various adsorbents. A review. Journal of Environmental Management. 2020;261:110236. doi:doi.org/10.1016/j.jenvman.2020.110236.

13. Daraei H, Mittal A. Investigation of adsorption performance of activated carbon prepared from waste tire for the removal of methylene blue dye from wastewater. Desalination and Water Treatment. 2017;90:294-8. doi:doi.org/10.5004/dwt.2017.21344.

14. Anastopoulos I, Mittal A, Usman M, Mittal J, Yu G, Núñez-Delgado A, Kornaros M. A review on halloysite-based adsorbents to remove pollutants in water and

wastewater. Journal of Molecular Liquids. 2018;269:855-68. doi:doi.org/10.1016/j.molliq.2018.08.104.

15. Kårelid V, Larsson G, Björlenius B. Pilot-scale removal of pharmaceuticals in municipal wastewater: Comparison of granular and powdered activated carbon treatment at three wastewater treatment plants. Journal of Environmental Management. 2017;193:491-502. doi:doi.org/10.1016/j.jenvman.2017.02.042.

16. De Andrade JR, Oliveira MF, Da Silva MGC, Vieira MGA. Adsorption of Pharmaceuticals from Water and Wastewater Using Nonconventional Low-Cost Materials: A Review. Industrial and Engineering Chemistry Research. 2018;57(9):3103-27. doi:10.1021/acs.iecr.7b05137.

17. Moreno-Castilla C. Adsorption of organic molecules from aqueous solutions on carbon materials. Carbon. 2004;42(1):83-94. doi:10.1016/J.CARBON.2003.09.022.

18. Calisto V, Ferreira CI, Oliveira JA, Otero M, Esteves VI. Adsorptive removal of pharmaceuticals from water by commercial and waste-based carbons. J Environ Manage. 2015;152:83-90. doi:10.1016/j.jenvman.2015.01.019.

19. Guillossou R, Le Roux J, Mailler R, Vulliet E, Morlay C, Nauleau F, Gasperi J, Rocher V. Organic micropollutants in a large wastewater treatment plant: What are the benefits of an advanced treatment by activated carbon adsorption in comparison to conventional treatment? Chemosphere. 2019;218:1050-60. doi:10.1016/j.chemosphere.2018.11.182.

20. Godino-Salido ML, López-Garzón R, Gutiérrez-Valero MD, Arranz-Mascarós P, Melguizo-Guijarro M, López de la Torre MD, Gómez-Serrano V, Alexandre-Franco M, Lozano-Castelló D, Cazorla-Amorós D, Domingo-García M. Effect of the surface chemical groups of activated carbons on their surface adsorptivity to aromatic

adsorbates based on π-π interactions. Materials Chemistry and Physics. 2014;143(3):1489-99. doi:10.1016/j.matchemphys.2013.12.005.

21. Sekulic MT, Boskovic N, Slavkovic A, Garunovic J, Kolakovic S, Pap S. Surface functionalised adsorbent for emerging pharmaceutical removal: Adsorption performance and mechanisms. Process Safety and Environmental Protection. 2019;125:50-63. doi:doi:10.1016/j.psep.2019.03.007.

22. Jaria G, Lourenço MAO, Silva CP, Ferreira P, Otero M, Calisto V, Esteves VI. Effect of the surface functionalization of a waste-derived activated carbon on pharmaceuticals' adsorption from water. Journal of Molecular Liquids. 2020;299:112098. doi:10.1016/j.molliq.2019.112098.

23. Jaria G, Silva CP, Oliveira JABP, Santos SM, Gil MV, Otero M, Calisto V, Esteves VI. Production of highly efficient activated carbons from industrial wastes for the removal of pharmaceuticals from water-A full factorial design. Journal of Hazardous Materials. 2019;370:212-8. doi:10.1016/j.jhazmat.2018.02.053.

24. Brunauer S, Emmett PH, Teller E. Adsorption of Gases in Multimolecular Layers. Journal of the American Chemical Society. 1938;60:309-19.

25. Dubinin MM. Properties of active carbons, In: Chemistry and Physics of Carbon. New York: Marcel Dekker Inc.; 1966.

26. Chung H-K, Kim W-H, Park J, Cho J, Jeong T-Y, Park P-K. Application of Langmuir and Freundlich isotherms to predict adsorbate removal efficiency or required amount of adsorbent. Journal of Industrial and Engineering Chemistry. 2015;28:241–6. doi:doi.org/10.1016/j.jiec.2015.02.021.

27. Lagergren S. Zur theorie der sogenannten adsorption gelöster stoffe. Kungliga Svenska Vetenskapsakademiens. Handlingar. 1898;24(4):1-39.

28. Ho YS, McKay G. Pseudo-second order model for sorption processes. Process Biochemistry. 1999; 34 451–65.

29. Limousin G, Gaudet JP, Charlet L, Szenknect S, Barthès V, Krimissa M. Sorption isotherms: A review on physical bases, modeling and measurement. Applied Geochemistry. 2007;22(2):249-75. doi:10.1016/j.apgeochem.2006.09.010.

30. Saha P, Chowdhury S. Insight Into Adsorption Thermodynamics, Thermodynamics, Mizutani Tadashi, IntechOpen, DOI: 10.5772/13474. Available from: https://www.intechopen.com/books/thermodynamics/insight-into-adsorption-thermodynamics. 2011.

31. Mourid EH, Lakraimi M, Benaziz L, Elkhattabi EH, Legrouri A. Wastewater treatment test by removal of the sulfamethoxazole antibiotic by a calcined layered double hydroxide. Applied Clay Science. 2019;168:87-95. doi:10.1016/j.clay.2018.11.005.

32. Atkins PW. Físico-Química (Tradução: Horacio Macedo). 6 ed. Rio de Janeiro, Brazil: LTC Editora; 1999.

33. Lima EC, Hosseini-Bandegharaei A, Moreno-Piraján JC, Anastopoulos I. A critical review of the estimation of the thermodynamic parameters on adsorption equilibria. Wrong use of equilibrium constant in the Van't Hoof equation for calculation of thermodynamic parameters of adsorption. Journal of Molecular Liquids. 2019;273:425-34. doi:10.1016/j.molliq.2018.10.048.

34. Ghosal PS, Gupta AK. Determination of thermodynamic parameters from Langmuir isotherm constant-revisited. Journal of Molecular Liquids. 2017;225:137–46 doi:doi.org/10.1016/j.molliq.2016.11.058.

35. Spessato L, Bedin KC, Cazetta AL, Souza IPAF, Duarte VA, Crespo LHS, Silva MC, Pontes RM, Almeida VC. KOH-super activated carbon from biomass waste:

Insights into the paracetamol adsorption mechanism and thermal regeneration cycles. Journal of Hazardous Materials. 2019;371:499-505.

36. Coates J. Interpretation of Infrared Spectra, A Practical Approach. Encyclopedia of Analytical Chemistry. Chichester: John Wiley & Sons Ltd; 2000.

37. Silverstein RM, Webster FX. Identificação Espectrométrica de Compostos Orgânicos. 6ª ed. Rio de Janeiro: LTC Livros Técnicos e Científicos; 2000.

38. Çalışır Ü, Çiçek B. Synthesis of thiol-glycol-functionalized carbon nanotubes and characterization with FTIR, TEM, TGA, and NMR technics. Chemical Papers. 2020;74:3293–302. doi:doi.org/10.1007/s11696-020-01152-6.

39. Aldewachi H, Woodroofe N, Gardiner P. Study of the Stability of Functionalized GoldNanoparticles for the Colorimetric Detection of Dipeptidyl Peptidase IV. Applied Sciences. 2018;8:2589. doi:doi:10.3390/app8122589.

40. Nielsen L, Biggs MJ, Skinner W, Bandosz TJ. The effects of activated carbon surface features on the reactive adsorption of carbamazepine and sulfamethoxazole. Carbon. 2014;80:419-32. doi:10.1016/j.carbon.2014.08.081.

41. Velo-Gala I, López-Peñalver JJ, Sánchez-Polo M, Rivera-Utrilla J. Surface modifications of activated carbon by gamma irradiation. Carbon. 2014;67:236-49. doi:10.1016/j.carbon.2013.09.087.

42. Deryło-Marczewska A, Skrzypczyńska K, Kuśmierek K, Świątkowski A, Zienkiewicz-Strzałka M. The adsorptive properties of oxidized activated carbons and their applications as carbon paste electrode modifiers. Adsorption. 2019;25:357–66 doi:doi.org/10.1007/s10450-019-00016-6.

43. Ma X, Yang H, Yu L, Chen Y, Li Y. Preparation, surface and pore structure of high surface area activated carbon fibers from bamboo by steam activation. Materials. 2014;7(6):4431-41. doi:10.3390/ma7064431.

44. Wang G, Wang H, Lu X, Ling Y, Yu M, Zhai T, Tong Y, Li Y. Solid-State Supercapacitor Based on Activated Carbon Cloths Exhibits Excellent Rate Capability. Advanced Materials 2014;26:2676–82.

45. Lee MS, Park M, Kim HY, Park SJ. Effects of Microporosity and Surface Chemistry on Separation Performances of N-Containing Pitch-Based Activated Carbons for CO2/N2 Binary Mixture. Scientific Reports. 2016;6(March):1-11. doi:10.1038/srep23224.

46. Li Z, Xu Z, Wang H, Ding J, Zahiri B, Holt CMB, Tan X, Mitlin D. Colossal pseudocapacitance in a high functionality–high surface area carbon anode doubles the energy of an asymmetric supercapacitor. Energy & Environmental Science. 2014;7(5):1708. doi:10.1039/c3ee43979h.

47. Martín-García B, Polovitsyn A, Prato M, Moreels I. Efficient charge transfer in solution-processed PbS quantum dot–reduced graphene oxide hybrid materials. J Mater Chem C. 2015;3:7088-95.

48. Roberts AD, Li X, Zhang H. Hierarchically porous sulfur-containing activated carbon monoliths via ice-templating and one-step pyrolysis. Carbon. 2015;95:268-78. doi:10.1016/j.carbon.2015.08.004.

49. Acosta R, Fierro V, Yuso AMd, Nabarlatz D, Celzard A. Tetracycline adsorption onto activated carbons produced by KOH activation of tyre pyrolysis char. Chemosphere. 2016;149:168-76. doi:doi.org/10.1016/j.chemosphere.2016.01.093.

50. Ndagijimana P, Liu X, Yu G, Wang Y. Synthesis of a novel core-shell-structure activated carbon material and its application in sulfamethoxazole adsorption. Journal of Hazardous Materials. 2019;368:602-12. doi:doi.org/10.1016/j.jhazmat.2019.01.093.

51. Liu Y, Liu X, Zhang G, Du TMT, Yang Y, Lu S, Wang W. Adsorptive removal of sulfamethazine and sulfamethoxazole from aqueous solution by hexadecyl trimethyl

ammonium bromide modified activated carbon. Colloids and Surfaces A: Physicochemical and Engineering Aspects. 2019;564:131-41. doi:doi.org/10.1016/j.colsurfa.2018.12.041.

52. Tonucci MC, Gurgel LVA, Aquino SFd. Activated carbons from agricultural byproducts (pine tree and coconut shell), coal, and carbon nanotubes as adsorbents for removal of sulfamethoxazole from spiked aqueous solutions: Kinetic and thermodynamic studies. Industrial Crops and Products. 2015;74:111-21. doi:doi.org/10.1016/j.indcrop.2015.05.003.

53. Moral-Rodríguez AI, Leyva-Ramos R, Ocampo-Pérez R, Mendoza-Barron J, Serratos-Alvarez IN, Salazar-Rabago. Removal of ronidazole and sulfamethoxazole from water solutions by adsorption on granular activated carbon: equilibrium and intraparticle diffusion mechanisms. Adsorption. 2016;22:89-103. doi:doi.org/10.1007/s10450-016-9758-0.

54. Miller JN, Miller JC. Statistics and Chemometrics for Analytical Chemistry. Sixth ed. England: Prentice Hall; 2010.

55. Travália BM, Forte MBS. New Proposal in a Biorefinery Context: Recovery of Acetic and Formic Acids by Adsorption on Hydrotalcites. Journal of Chemical & Engineering Data. 2020;65(9):4503-11. doi:DOI: 10.1021/acs.jced.0c00340.

56. Hong S, Wen C, He J, Gan F, Ho YS. Adsorption thermodynamics of Methylene Blue onto bentonite. J Hazard Mater. 2009;167(1-3):630-3. doi:10.1016/j.jhazmat.2009.01.014.

57. Subramani SE, Thinakaran N. Isotherm, kinetic and thermodynamic studies on the adsorption behaviour of textile dyes onto chitosan. Process Safety and Environmental Protection. 2017;106:1-10. doi:10.1016/j.psep.2016.11.024.

58. Tran HN, You S-J, Chao H-P. Thermodynamic parameters of cadmium adsorption onto orange peel calculated from various methods: A comparison study. Journal of Environmental Chemical Engineering. 2016;4(3):2671-82. doi:doi.org/10.1016/j.jece.2016.05.009.

59. Ahmed MB, Zhou JL, Ngo HH, Guo W. Adsorptive removal of antibiotics from water and wastewater: Progress and challenges. Science of The Total Environment. 2015;532:112-26. doi:10.1016/J.SCITOTENV.2015.05.130.

60. Coimbra RN, Calisto V, Ferreira CIA, Esteves VI, Otero M. Removal of pharmaceuticals from municipal wastewater by adsorption onto pyrolyzed pulp mill sludge. Arabian Journal of Chemistry. 2019;12(8):3611-20. doi:doi.org/10.1016/j.arabjc.2015.12.001.

61. Silva CP, Jaria G, Otero M, Esteves VI, Calisto V. Adsorption of pharmaceuticals from biologically treated municipal wastewater using paper mill sludge-based activated carbon. Environ Sci Pollut Res Int. 2019;26(13):13173-84. doi:10.1007/s11356-019-04823-w.

62. Ahmed MB, Zhou JL, Ngo HH, Guo W, Johir MAH, Belhaj D. Competitive sorption affinity of sulfonamides and chloramphenicol antibiotics toward functionalized biochar for water and wastewater treatment. Bioresour Technol. 2017;238:306-12. doi:10.1016/j.biortech.2017.04.042.

63. Bonvin F, Jost L, Randin L, Bonvin E, Kohn T. Super-fine powdered activated carbon (SPAC) for efficient removal of micropollutants from wastewater treatment plant effluent. Water Research. 2016;90:90-9. doi:doi.org/10.1016/j.watres.2015.12.001.

64. Akpotu SO, Moodley B. Encapsulation of Silica Nanotubes from Elephant Grass with Graphene Oxide/Reduced Graphene Oxide and Its Application in Remediation of

Sulfamethoxazole from Aqueous Media. ACS Sustainable Chemistry and Engineering. 2018;6(4):4539-48. doi:doi.org/10.1021/acssuschemeng.7b02861.

Figure 1. Pore size distribution determined for AC-P (grey line) and AC-MPTMS (black line).

Figure 2. XPS high-resolution spectra (with deconvolution) of C1s, O1s, N1s and Si2s+S2p determined for AC-P (left) and AC-MPTMS (right).

Figure 3. Experimental results from the kinetic (1) and equilibrium (2) studies on the adsorption of SMX from ultrapure buffered water (pH 8) onto a) AC-P and b) AC-MPTMS at three different temperatures (15, 25 and 35 ºC). Kinetic and equilibrium experimental results are represented together with fittings to the PSO model and Langmuir model, respectively.

Figure 4. Experimental results from the a) kinetic and b) equilibrium studies on the adsorption of SMX onto AC-MPTMS from wastewater (at 25 ºC) together with fittings to the considered models.

Table 1. Fitting results from the kinetic and equilibrium studies on the adsorption of SMX onto AC-P and AC-MPTMS from ultrapure buffered water (pH 8) at three different temperatures (15, 25 and 35 ^{o}C).

Model / Parameter	**Adsorbent**					
	AC-P			**AC-MPTMS**		
	Temperature			**Temperature**		
	288 K (15 ºC)	**298 K (25 ºC)**	**308 K (35 ºC)**	**288 K (15 ºC)**	**298 K (25 ºC)**	**308 K (35 ºC)**
Kinetic fittings						
Pseudo-first order						
q_e (mg g^{-1})	97 ± 4	89 ± 3	58.1 ± 0.6	50 ± 2	53 ± 2	37.2 ± 0.9
k_1 (min^{-1})	0.3 ± 0.1	0.3 ± 0.1	0.30 ± 0.03	0.20 ± 0.05	0.30 ± 0.08	0.40 ± 0.09
R^2	0.915	0.939	0.994	0.914	0.940	0.977
Pseudo-second order						
q_e (mg g^{-1})	101 ± 4	93 ± 2	59.1 ± 1.2	52 ± 2	55.0 ± 1.4	37.6 ± 0.9
k_2 (g mg^{-1} min^{-1})	0.005 ± 0.002	0.006 ± 0.002	0.013 ± 0.004	0.006 ± 0.002	0.009 ± 0.003	0.03 ± 0.01
R^2	0.950	0.971	0.983	0.959	0.974	0.980

			Isotherm fittings			
Langmuir						
q_m (mg g^{-1})	113 ± 7	62 ± 3	42.5 ± 0.6	140 ± 20	48.9 ± 1.4	28.0 ± 1.5
K_L (L mg^{-1})	4.2 ± 1.2	19 ± 6	26 ± 4	0.24 ± 0.06	1.3 ± 0.1	1.9 ± 0.4
R^2	0.971	0.960	0.997	0.983	0.996	0.978
Freundlich						
n	6 ± 2	16 ± 8	11 ± 3	1.51 ± 0.09	3.2 ± 0.3	3.9 ± 0.8
K_F ($mg^{1-1/n}$ $L^{1/n}$ g^{-1})	88 ± 4	55 ± 2	39.2 ± 0.9	28.2 ± 1.1	27.1 ± 0.9	18.1 ± 0.7
R^2	0.943	0.940	0.989	0.988	0.987	0.961

Table 2. Thermodynamic parameters calculated for the adsorption of SMX onto AC-P and AC-MPTMS.

Carbon material	**Temperature (K)**	**Activation energy, E_a (kJ mol^{-1})**	**Pre-exponential factor, A (g mg^{-1} min^{-1})**	**Isotherm model**	***ΔG°* (kJ mol^{-1}) ***	***ΔH°* (kJ mol^{-1})**	***ΔS°* (J mol^{-1} K^{-1})**
AC-P	288	36 ± 13	$1.6x10^{4}$ ± $2.9x10^{4}$	*Langmuir*	-33.2 ± 0.2	68.9 ± 0.4	356 ± 88
	298				-38.1 ± 0.3		
	308				-40.20 ± 0.06		
AC-MPTMS	288	61 ± 17	$5.6x10^{8}$ ± $6.3x10^{4}$	*Langmuir*	-26.4 ± 0.2	78.2 ± 0.4	365 ± 96
	298				-31.48 ± 0.02		
	308				-33.5 ± 0.1		

* The value of ΔG^o was calculated by equation (3) $\Delta G^o = -RT \ln K_e$

Table 3. Fitting results for the kinetic and equilibrium studies on the adsorption of SMX onto AC-MPTMS from wastewater (at 25 ºC).

Kinetic fittings Model/parameter		**Isotherm fittings Model/parameter**	
Pseudo-first order		***Langmuir***	
q_e (mg g^{-1})	18.6 ± 1.1	q_m (mg g^{-1})	16.1 ± 0.3
k_1 (min^{-1})	0.06 ± 0.02	K_L (L mg^{-1})	3.8 ± 0.4
R^2	0.866	R^2	0.996
Pseudo-second order		***Freundlich***	
q_e (mg g^{-1})	19.69 ± 0.98	n	6.2 ± 0.6
k_2 (g mg^{-1} min^{-1})	0.004 ± 0.002	K_F ($mg^{1-1/n}$ $L^{1/n}$ g^{-1})	12.4 ± 0.2
R^2	0.925	R^2	0.995

Graphical abstract

Highlights

- Waste-based activated carbon (AC-P) was functionalized with thiol groups (AC-MPTMS)
- AC-P and AC-MPTMS were tested for the adsorption of sulfamethoxazole (SMX) from water
- AC-P attained equal (at 15 ^{o}C) or larger (at 25 and 35 ^{o}C) Langmuir q_m than AC-MPTMS
- For both AC-P and AC-MPTMS, Langmuir q_m decreased with temperature while K_L increased
- Activation energy was slightly lower for SMX adsorption onto AC-P than onto AC-MPTMS

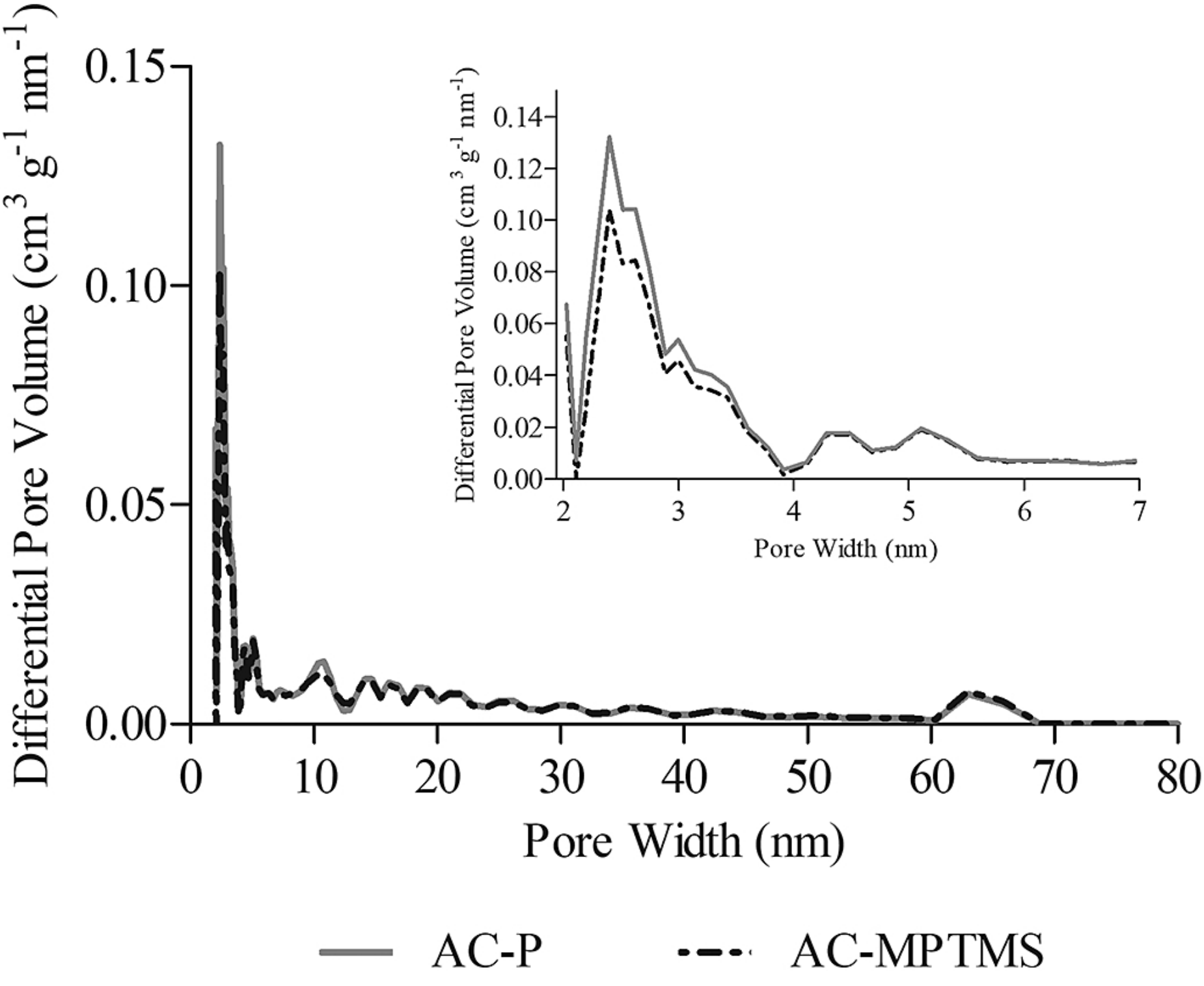
Differential Pore Volume (cm^3 g^{-1} nm^{-1})
0.15
0.10
0.05
0.00
0
10
20
30
40
50
60
70
80
Pore Width (nm)
Differential Pore Volume (cm^3 g^{-1} nm^{-1})
0.14
0.12
0.10
0.08
0.06
0.04
0.02
0.00
2
3
4
5
6
7
Pore Width (nm)
AC-P
AC-MPTMS

Figure 1

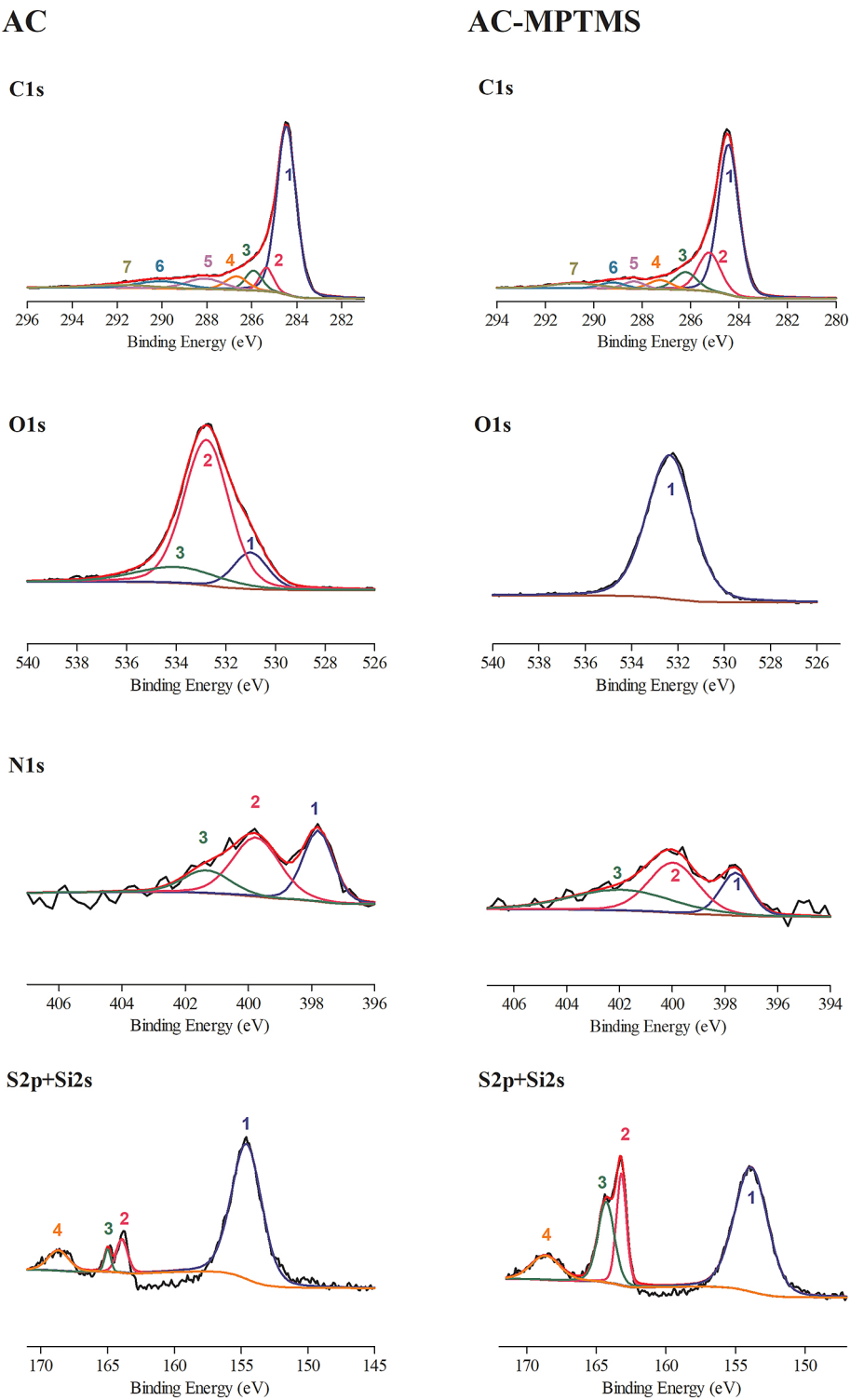
AC
AC-MPTMS
C1s
C1s
O1s
O1s
N1s
S2p+Si2s
S2p+Si2s
Binding Energy (eV)

Figure 2

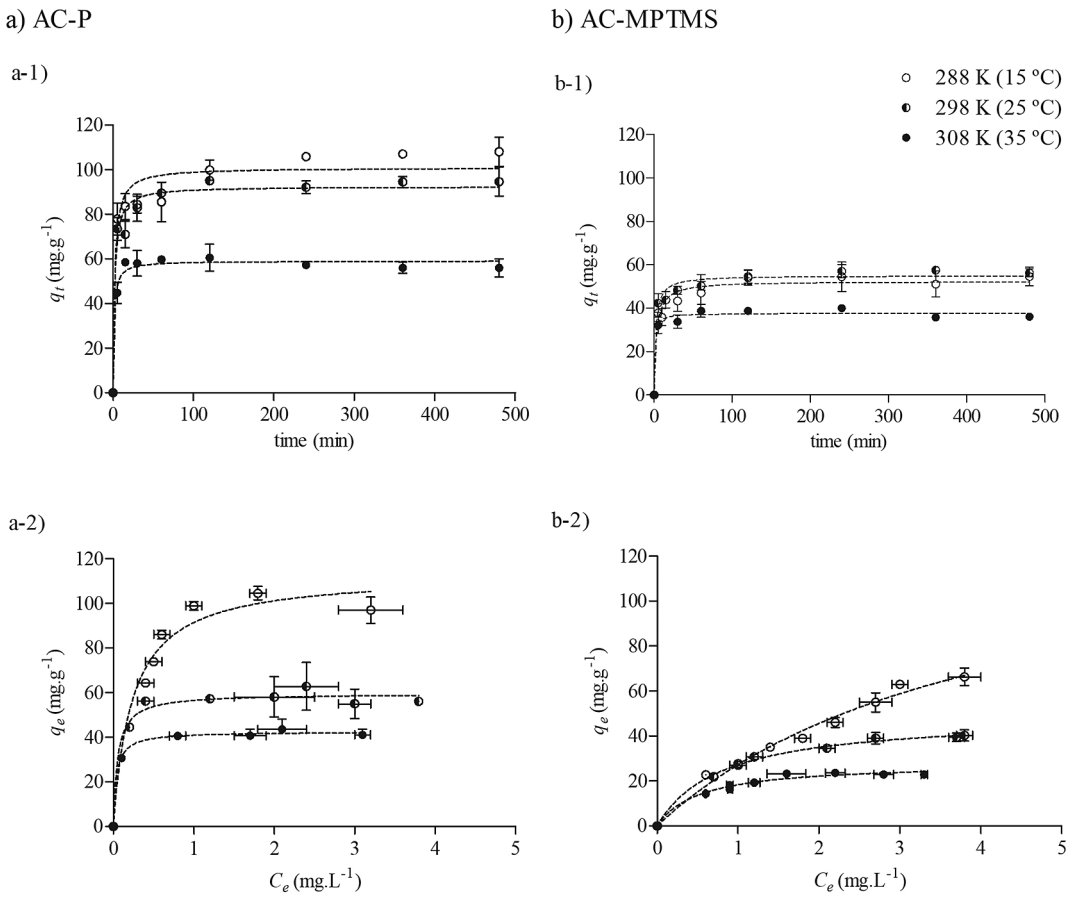
a) AC-P
b) AC-MPTMS
a-1)
b-1)
288 K (15 ºC)
298 K (25 ºC)
308 K (35 ºC)
q_t (mg.g^{-1})
time (min)
a-2)
b-2)
q_e (mg.g^{-1})
C_e (mg.L^{-1})

Figure 3

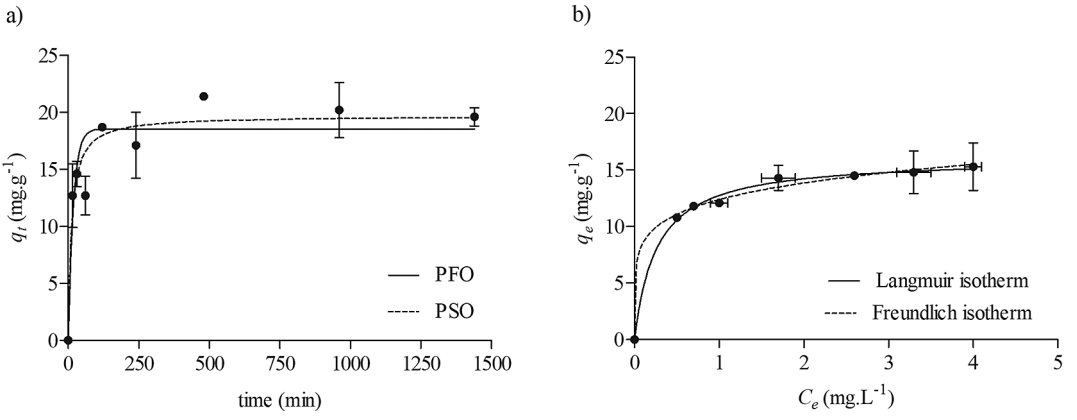
a)
b)
q_t (mg.g^{-1})
time (min)
PFO
PSO
q_e (mg.g^{-1})
C_e (mg.L^{-1})
Langmuir isotherm
Freundlich isotherm

Figure 4